Journal of Fluids and Structures 54 (2015) 263–280

Contents lists available at ScienceDirect

Journal of Fluids and Structures

journal homepage: www.elsevier.com/locate/jfs

Transverse galloping of circular cylinders fitted with solid and slotted splitter plates

Gustavo R.S. Assi [a,*], Peter W. Bearman [b]

[a] Dept. of Naval Arch. & Ocean Eng., University of São Paulo, São Paulo, Brazil
[b] Department of Aeronautics, Imperial College, London, UK

ARTICLE INFO

Article history:
Received 8 May 2014
Accepted 1 November 2014
Available online 6 December 2014

Keywords:
Flow-induced vibration
Galloping
Circular cylinder
Splitter plate

ABSTRACT

The galloping response of a circular cylinder fitted with three different splitter plates and free to oscillate transverse to a free stream has been investigated considering variations in plate length and plate porosity. Models were mounted in a low mass and damping elastic system and experiments have been carried out in a recirculating water channel in the Reynolds number range of 1500 to 16 000. Solid splitter plates of 0.5 and 1.0 diameter in length are shown to produce severe galloping responses, reaching displacements of 1.8 diameters in amplitude at a reduced velocity of around 8. Fitting a slotted plate with a porosity ratio of 30% also caused considerable vibration, but with a reduced rate of increase with flow speed. All results are compared with the typical vortex-induced vibration response of a plain cylinder. Force decomposition in relation to the body velocity and acceleration indicates that a galloping mechanism is responsible for extracting energy from the flow and driving the oscillations. Visualisation of the flow field around the devices performed with PIV reveal that the reattachment of the free shear layers on the tip of the plates is the hydrodynamic mechanism driving the excitation.

1. Introduction

The study of bluff bodies fitted directly with splitter plates or in the presence of splitter plates is not new. Experiments performed by Roshko (1954), Bearman (1965) and Gerrard (1966) with a variety of bluff bodies report significant changes in base pressure, vortex formation length and Strouhal number depending on the length of a splitter plate and the distance it is positioned downstream of the body. From the attenuation of vibration of offshore risers to the reduction of noise from an aeroplane's landing gear, previous studies are mainly concerned with the suppression of vortex shedding.

The present investigation was motivated by the use of a splitter plate as a means to suppress vortex-induced vibration (VIV) of offshore risers, which are characterised by highly flexible pipes with relatively low mass and damping susceptible to excitation by ocean currents. In contrast, if the purpose is to enhance vibrations of a low mass-damping system (Chang et al., 2011, for example), the addition of splitter plates may produce considerable improvement in the response for the same range of flow speeds. Cylinders with splitter plates or fitted with other devices prone to galloping may be useful if employed to harvest energy from the flow.

* Correspondence to: NDF Research Group – Dept. Eng. Naval e Oceânica, Escola Politécnica da Universidade de São Paulo, Av. Prof Mello Moraes 2231, 05508-030, São Paulo - SP, Brazil.
E-mail address: g.assi@usp.br (G.R.S. Assi).
URL: http://www.ndf.poli.usp.br (G.R.S. Assi).

http://dx.doi.org/10.1016/j.jfluidstructs.2014.11.005
0889-9746/

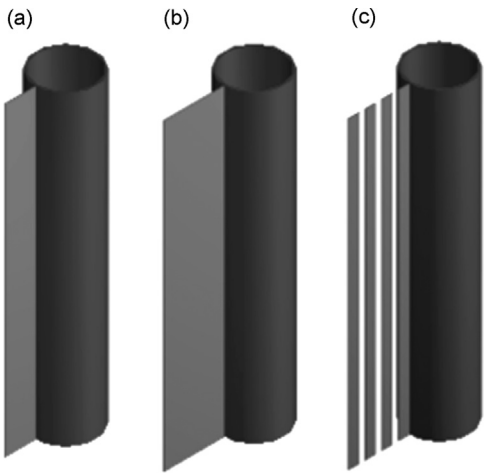

Fig. 1. Representation of tested devices: (a) solid splitter plate $L/D=0.5$, (b) solid splitter plate $L/D=1.0$ and (c) slotted splitter plate $L/D=1.0$.

It is known that if vortex shedding from a fixed cylinder is eliminated, say by the use of a long splitter plate (Cimbala and Garg, 1991), then drag is reduced. Hence conceptually an effective VIV suppression device should be able to reduce drag rather than increase it. Assi et al. (2009) have shown that suppression of cross-flow and streamwise VIV of a circular cylinder, with resulting drag coefficients less than that for a fixed plain cylinder, can be achieved using two-dimensional control plates in low mass-damping systems. A free-to-rotate splitter plate was found to suppress VIV, but instead of remaining aligned with the flow on the centreline of the wake the plate adopted a stable but deflected position when it was released. Cimbala and Garg (1991) had also observed such a bi-stable behaviour of the plate for a free-to-rotate cylinder fitted with a splitter plate.

Successful VIV suppression has been achieved with splitter plates for systems with one and two degrees of freedom as reported by Assi et al. (2009, 2010a). In their experiments the plate was free to rotate to allow for the device to realign itself with the incoming flow, thus producing a omni-directional suppressor. However, when non-rotating splitter plates (among other devices) were investigated it was found that they induced the system into severe galloping-type responses instead of suppressing VIV. Although a failure in VIV suppression, we find such behaviour very interesting and worthy of a detailed investigation.

Therefore, the present study will focus on the comparison between the flow-induced vibration (FIV) of a plain circular cylinder and a cylinder fitted with non-rotating splitter plates with different lengths and porosities, as illustrated in Fig. 1.

1.1. Classical galloping of non-circular cross sections

The term *galloping* has been generally employed to describe a specific type of FIV mechanism that occurs for bodies moving in one degree of freedom (1-dof) with non-circular cross sections. Comprehensive reviews of the classical theory of galloping have been written by Parkinson (1971, 1989), Blevins (1990), Naudascher and Rockwell (1994) and Paidoussis et al. (2011). Classical galloping of non-circular cylinders (the square section being the classic example) is caused by a fluid-dynamic instability of the cross section of the body such that the motion of the structure generates forces which increase the amplitude of vibration (Bearman et al., 1987).

We will argue that a galloping mechanism similar to that occurring in a square cross-section takes place when an elastically mounted cylinder with a non-rotating splitter plate is placed in an oncoming flow.

If a perturbation displaces the body from rest the relative velocity of the flow will be the vectorial sum of the oncoming flow speed, U, and the body's velocity, $\dot{y}$, defining an angle of incidence, α, in relation to the free stream. As depicted in Fig. 2, the upper shear layer approaches the body surface whereas the lower shear layer moves away. Depending on plate length and the body's movement, the separated shear layers will tend to reattach to the tip of the plates as the cylinder oscillates. This generates a decrease in pressure on the upper surface and an increase on the lower surface leading to a transverse fluid force, F_y, acting in the same direction as the motion and causing an increase in the displacement. The stiffness of the spring will eventually act to restore the body back to its original position. When the body reaches its maximum displacement and $\dot{y}$ then changes direction the process is inverted, though with F_y still acting in the same direction as $\dot{y}$. Therefore, in the classical galloping mechanism the cross-flow fluid force is *in phase* with the body's velocity, acting as a negative damping term in the equation of motion, hence classical galloping is classified as a damping-controlled fluid-elastic mechanism. The magnitude of F_y increases with α, which itself increases with $\dot{y}$, resulting in a continuous increase in the steady state amplitude of vibration with increasing flow speed.

"For while VIV is typically limited to amplitudes less than $1D$, galloping amplitudes can be many times D" (Parkinson, 1971). Of course a vortex wake will develop further downstream of a square section or a cylinder with splitter plate as in any

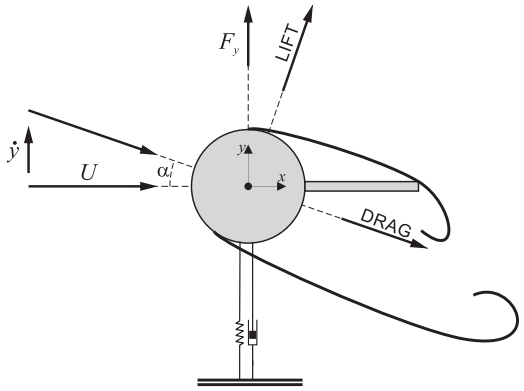

Fig. 2. Proposed sketch of flow and hydrodynamic forces for galloping of a cylinder with splitter plate.

other bluff body, but the galloping instability is not a resonant mechanism that depends on matching values of natural frequency, f_0, and the vortex shedding frequency, f_s. For this reason classical galloping allows for modelling with a quasi-steady approach considering that the fluid force on the structure is assumed to be determined solely by the instantaneous relative velocity. "The quasi-steady assumption is valid only if the frequency of periodic components of fluid force, associated with vortex shedding or time-lag effects, is well above the vibration frequency of the structure ($f_s \gg f_0$)" (Blevins, 1990). This is generally the case for high values of reduced velocity, defined as the flow speed non-dimensionalised by cylinder diameter and natural frequency. Of course a square section bluff body is also susceptible to VIV at low reduced velocities, however this may be combined with a galloping excitation which will persist for velocities above the resonant range for VIV. "While vortex-induced oscillations occur only in discrete ranges of [flow] speed, galloping will occur at all flow speeds above a critical value determined by the structural damping" (Parkinson, 1971).

Parkinson (1971), referring to den Hartog (1956), presents a simplified quasi-steady analysis that is very useful in predicting the stability of a 1-dof system to classical galloping. The so called 'galloping stability criterion' is evaluated be measuring force coefficients on the body for various incidence angles in a steady flow. The reader is encouraged to read Paidoussis et al. (2011) and the above references for further details.

By balancing the negative damping generated by F_y and the structural damping it is possible to determine the critical reduced velocity for the onset of galloping. Depending on the parameters of mass ratio (m^*, defined as the ratio of structural mass to the mass of displaced fluid) and damping (ζ, calculated as a fraction of critical damping), galloping instability can appear for relatively low reduced velocities, overlapping with the VIV range.

Blevins (1990) writes that "the major limitation of the [classical] galloping theory is that the aerodynamic coefficients are assumed to vary only with angle of attack, but experience shows that the coefficients are affected by turbulence and vortex shedding." He states that the quasi-steady assumption employed in this analysis requires that the vortex shedding frequency be well above the natural frequency so that "the fluid responds quickly to any structural motion". Based on experimental works found in the literature he concluded that "the reduced velocity must exceed 20 and the amplitude of vibration should not exceed 0.1 to 0.2D for application of the quasi-steady theory." This conclusion was also reached by Nakamura et al. (1994). Since this is not the case in the present investigation, the classical galloping criterion will not be verified in the present work.

1.2. Previous experiments of cylinders with splitter plates

A few experiments with static cylinders fitted with splitter plates have been performed in the past and could throw some light in the hydrodynamic mechanisms behind this investigation.

Apelt et al. (1973) performed experiments with a static cylinder fitted with a splitter plate of $L/D \leq 2.0$ (ratio of plate length to the cylinder diameter) in a water tunnel in the range of $\mathrm{Re} = 10^4$ to 5×10^4. They showed that the overall behaviour of the wake can be greatly affected when a splitter plate is placed in the near wake along the centreline. If separation points are stabilised, drag may be considerably reduced and a wake narrower than that for a plain cylinder is produced. They reported that minimum drag and Strouhal number were obtained when $L/D = 1.0$ and increased for other plate lengths. Later, the work was extended to plates with L/D between 2 and 7 in the same Re range (Apelt and West, 1975), with results indicating that no further changes are likely to be produced by lengthening the splitter plates beyond the limits tested. Bluff bodies other than circular cylinders have also been considered by Apelt and West (1975).

Unal and Rockwell (1987) performed experiments in the range of $\mathrm{Re} = 140$ to 3600 to investigate the control of the wake by the proximity of a splitter plate to the bluff body. The length of the plate was many times the diameter ($L/D = 24$), yielding only the gap between the cylinder and the plate as the governing parameter. The plate was not attached to the cylinder nor was the system free to respond with flow-induced vibrations, however this fine experiment clearly illustrated the sensitivity of the vortex formation mechanism to the interference of a plate positioned downstream of the near wake.

Suppressors that are free to rotate about the cylinder have the advantage of being omnidirectional, realigning their orientation as flow direction changes. They mitigate vibrations and reduce drag if a stable configuration is found. Particle-image velocimetry (PIV) measurements from Assi et al. (2009) showed that the shear layer separated from the cylinder appeared to attach to the tip of the plate on the same side to which the plate had deflected and this had the effect of stabilising the near-wake flow. Vortex shedding was visible downstream but this did not feed back to cause vibrations. An unwanted effect was the appearance of a steady transverse force on the cylinder towards the side to which the splitter plate had deflected. This steady lift could be eliminated by using a pair of splitter plates arranged so that the shear layers springing from both sides of the cylinder could attach to the tips of both plates. However, it is known that free-to-rotate splitter plates may experience hydrodynamic instabilities that will not only cause a substantial increase in drag but also prevent them from suppressing vibrations (Assi et al., 2009). Actually, an unstable free-to-rotate suppressor may induce the structure into very vigorous vibrations excited by a type of flutter mechanism. Assi et al. (2009, 2011) have shown that the instability of free-to-rotate suppressors is directly related to the level of rotational resistance encountered in the system as well as geometric parameters such as plate length. "Devices with rotational friction below a critical value oscillate themselves as the cylinder vibrates, sometimes increasing the amplitude of cylinder oscillation higher than that for a plain cylinder". On the other hand, if the rotational resistance is above a limiting threshold the suppressor cannot rotate and an undesired galloping response is initiated.

Free vibration experiments performed by Stappenbelt (2010) for a low aspect ratio cylinder fitted with splitter plates with $L/D \leq 4$ registered galloping response for a reduced velocity range between 3 and 60. For small L/D the response of the cylinder appeared to be strongly influenced by vortex shedding and an abrupt decrease in the galloping response occurred at higher reduced velocities. With increasing plate length "there appears to be a smooth transition from pure VIV to a galloping-type response heavily influenced by the vortex shedding at low reduced velocity and a predominantly galloping response at high reduced velocity". This is in agreement with experiments with splitter plates and other suppressors reported in Assi et al. (2011, 2014).

Nakamura et al. (1994) experimented with spring supported circular cylinders fitted with long splitter plates from $L/D=$ 4.2 to 31.3 in the range of $\mathrm{Re}=0.6\times10^4$ to 4.2×10^4 to show that plate length had a significant effect on the galloping instability. Plots of response amplitude versus reduced velocity were not obtained since they were more concerned with the onset of galloping by measuring small amplitudes and the growth rate of oscillation. Nevertheless, they highlighted the inapplicability of the quasi-steady theory of classical galloping to a cylinder fitted with a long splitter plate. Plotting static force coefficients versus incidence angle they found that $L/D=20.8$ produced a stable system. This was very different from the unstable behaviour observed during free vibration experiments. For a splitter plate with $L/D=4.2$ they found a stable system according to the galloping criterion, but still the classical quasi-steady theory could not predict the correct velocity for the onset of galloping. Similar results have been observed for a rectangular cylinder reported in Nakamura et al. (1991). Both papers together conclude that bluff bodies, with or without sharp edges, may gallop in the presence of a splitter plate.

In the present work we are concerned with the flow-induced response of cylinders fitted with much shorter plates of around $L/D=1$. This is the characteristic length for a device that could be employed in the suppression of flow-induced vibration of offshore structures, for example.

2. Experimental arrangement

Experiments were performed in the Department of Aeronautics at Imperial College using a recirculating water channel with a free surface and a test section 0.6 m wide, 0.7 m deep and 8.0 m long. Flow speed was continuously variable up to $U=0.6$m/s and free stream turbulence intensity across the section was around 3%. Circular cylinder models were made from a 50 mm diameter acrylic tube, giving a maximum $\mathrm{Re}=30\,000$, based on cylinder diameter D. With a wet-length of 650 mm

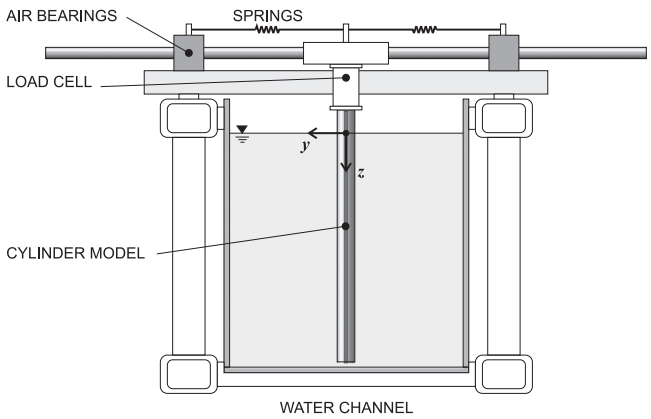

Fig. 3. Representation of the cylinder fitted with a splitter plate mounted on the 1-dof rig in the test section of the water channel. View of the cross-section.

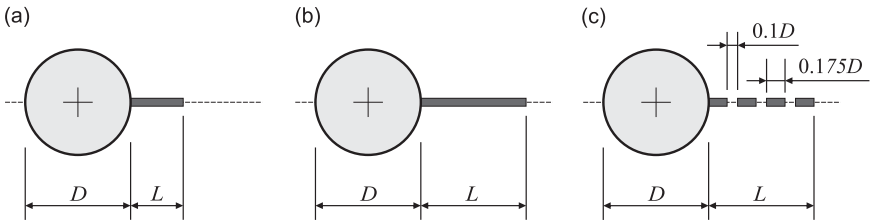

Fig. 4. Geometric parameters of tested devices: (a) solid splitter plate $L/D=0.5$, (b) solid splitter plate $L/D=1.0$ and (c) slotted splitter plate $L/D=1.0$.

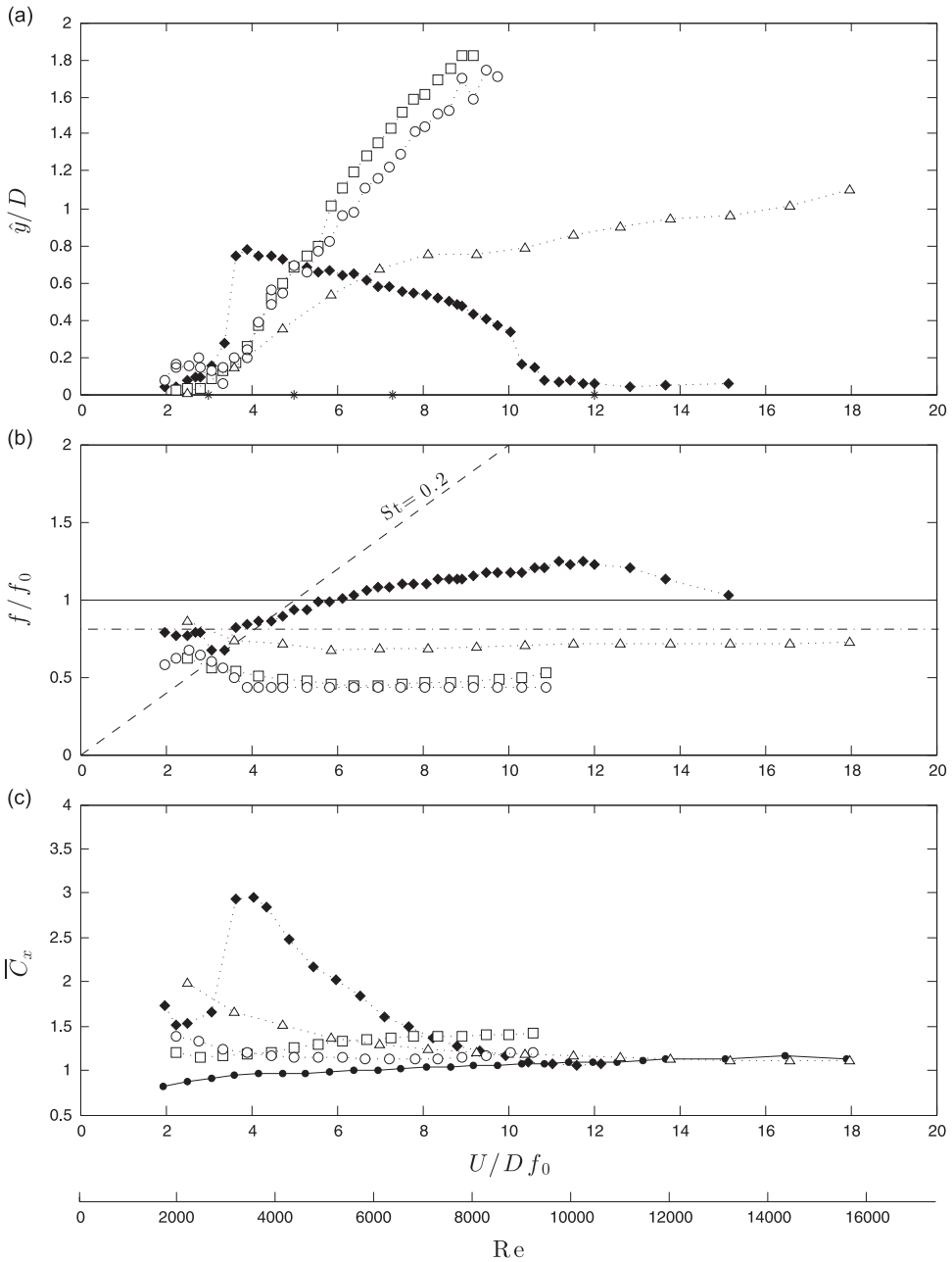

Fig. 5. Galloping response of cylinder fitted with non-rotating devices. (a) Displacement, (b) frequency and (c) mean drag coefficient versus reduced velocity. Key: ● static cylinder, ◊ plain cylinder VIV, □ solid splitter plate $L/D=0.5$, ○ solid splitter plate $L/D=1.0$, ▵ slotted plate $L/D=1.0$.

(total length below water level), the resulting aspect ratio of the model was 13. The cylinder was fixed at its upper end to a 1-dof (degree of freedom) elastic mounting represented in Fig. 3. The model was aligned in the vertical direction passing through the free surface and mounted such that there was a 2 mm gap between the lower end of the cylinder and the glass floor of the test section. It was judged preferable not to install end plates on the cylinder in order not to increase the fluid damping in the system. The support was firmly attached to the channel structure and sliding cylindrical guides were free to move in the transverse direction (y-axis) through air bearings. A pair of coil springs connecting the moving base to the fixed supports provided the restoration force for the system. The present setup has already been employed and validated in previous experiments (Assi et al., 2010a, 2010b, 2013; Assi, 2014a, 2014b).

It is known that the dynamic response of a cylinder is extremely sensitive to the structural characteristics of the system, so extra care was taken to determine the precise values of natural frequency, mass and damping of the structure. All moving parts of the elastic base contributed to the effective mass oscillating with the cylinder, resulting in a mass ratio of $m^* = 2.6$ (calculated as the total mass divided by the mass of displaced water). The air bearings proved to be an effective way to reduce damping without compromising the stiffness of the structure, especially in resisting drag loads for higher flow speeds. By carrying out free decay tests in air it was also possible to estimate the structural damping of the system resulting in $\zeta = 0.7\%$, calculated as a percentage of the critical damping, yielding the product $m^*\zeta = 0.018$.

A load cell was installed between the model and the platform to measure hydrodynamic forces acting on the cylinder and an optical positioning sensor measured the y-displacement without adding damping. A PIV system was employed to map velocity fields. More details about the experimental setup, flow quality, the design of the load cell and operation of the 1-dof rig can be found in Assi (2009).

Measurements were made using one set of springs and the reduced velocity range covered was from $U/Df_0 = 2$ to 20, where reduced velocity is defined using the cylinder natural frequency of oscillation, f_0, measured in air. The only flow variable changed during the course of the experiments was U, which alters both the reduced velocity and Reynolds number. Throughout the study, cylinder displacement amplitudes, $\hat{y}/D$, were found by measuring the root mean square value of response and multiplying by $\sqrt{2}$ (the so called harmonic amplitude). Displacements were nondimensionalised by dividing by D.

Three splitter plates were built out of acrylic plastic and installed on the cylinder model following the geometric parameters in Fig. 4. Two solid splitter plates with $L/D = 0.5$ and 1.0, shown in Fig. 4(a) and (b), were employed to evaluate the dependency of the response on plate length. A slotted plate with $L/D = 1.0$, shown in Fig. 4(c), was built in order to investigate the effect of plate porosity (or permeability) on the response. Parallel slots were cut out of the plate material creating 0.1D-wide continuous gaps in the vertical direction along the whole span of the cylinder (refer to Fig. 1(c)). The slotted plate presented 70% of the area of a completely solid plate of the same length, thus defining a porosity ratio of 30%. Plates were rigidly attached to the cylinders and aligned with the incoming flow direction, which is from left to right in Fig. 4. Plates were 3 mm thick ($0.06D$) and did not bend with the flow; their installation did not significantly alter m^*.

3. Results and discussion

Preliminary experiments performed with a plain cylinder will serve to serve the experimental setup and as a reference for the discussion that follows. During the typical VIV excitation, as U increases, the frequency of vortex-shedding, f_s, gets close enough to f_0 such that the unsteady pressure fluctuations in the near wake induce the body to respond. Once the cylinder starts to oscillate, the vibrations will control the vortex formation process and f_s becomes *locked in* to the response frequency, f, near f_0. If the velocity continues to increase f_s moves away from f_0 so that vortex shedding becomes uncoupled with the cylinder frequency. Refer to Williamson and Govardhan (2004) for a detailed description of the VIV mechanism and typical responses.

Depending on the mass of the system and the specific mass of the fluid in which the cylinder is immersed, the frequency of oscillation can be significantly influenced by the additional mass of fluid that is accelerated with the body. For this reason, the reduced mass parameter, m^* is relevant for the response of light cylinders immersed in water and, consequently, f_0 measured in air will be different from the natural frequency in still water, f_W. As expected, the response of a forced linear oscillator will be inversely proportional to the product of m^* and ζ (Bearman, 1984).

The typical VIV response of a plain cylinder, in terms of amplitude and frequency of oscillation, is presented in Fig. 5 and shows a good agreement with the results reviewed by Williamson and Govardhan (2004). Fig. 5(a) shows the typical resonant response of VIV in the displacement curve, with vibration building up in the synchronisation range between $U/Df_0 \approx 3.0$ and 11 and a maximum response of $\hat{y}/D = 0.8$ at $U/Df_0 \approx 4.0$. Fig. 5(b) shows the dominant frequency of response, f, normalised by f_0. The inclined dashed line represents a Strouhal number of 0.2, approximately equivalent to the vortex shedding frequency for a static cylinder. The horizontal dot-dashed line represents the natural frequency of the system measured in still water ($f_W/f_0 \approx 0.8$). Frequency measurements for $U/Df_0 > 11$ are kept in the plot but must be treated with caution, since beyond the end of the synchronisation range displacements are very small (below $\hat{y}/D = 0.1$) and the frequency spectrum becomes quite broad. Mean drag coefficient ($\overline{C}_x$) in Fig. 5(c) reveals the amplification of drag normally observed during the synchronisation range for VIV. A curve for the drag of a fixed cylinder (static) has also been added as a reference. Fluid force measurements are in good agreement with the results presented by Khalak and Williamson (1999).

3.1. Displacement, frequency and drag

Results for the cylinders fitted with splitter plates are presented together with results for the plain cylinder in Fig. 5. The first distinct difference, when compared against the plain cylinder VIV, is observed in the displacement curves in Fig. 5(a). All cylinders fitted with splitter plates show a continuous increase in response as flow speed is increased. Cylinders with solid splitter plates show a steeper response curve when compared with the slotted plate, but none respond with the resonant behaviour typical of VIV. In fact, the response curves for the two solid splitter plate cases are not very different,

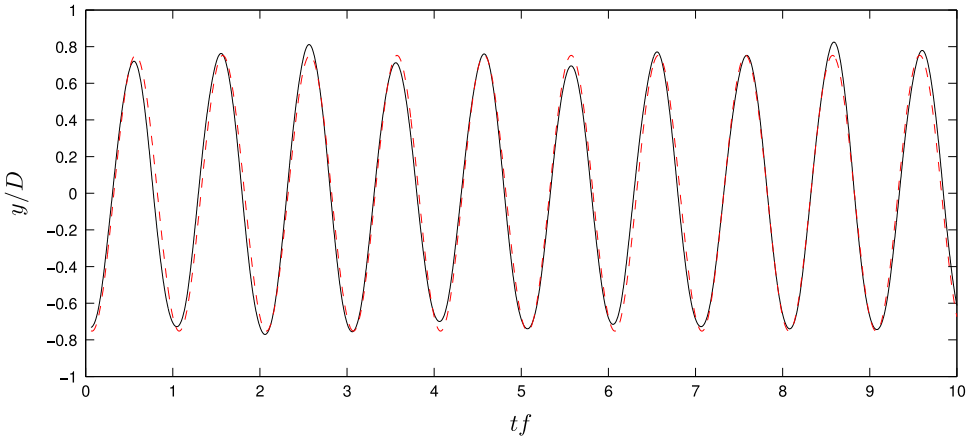

Fig. 6. Sample of displacement time series (continuous line) compared with a harmonic curve $y(t)=\hat{y}\sin(2\pi ft)$ (dashed line) for a cylinder fitted with a solid splitter plate with $L/D=1.0$ at $U/Df_0=8.1$.

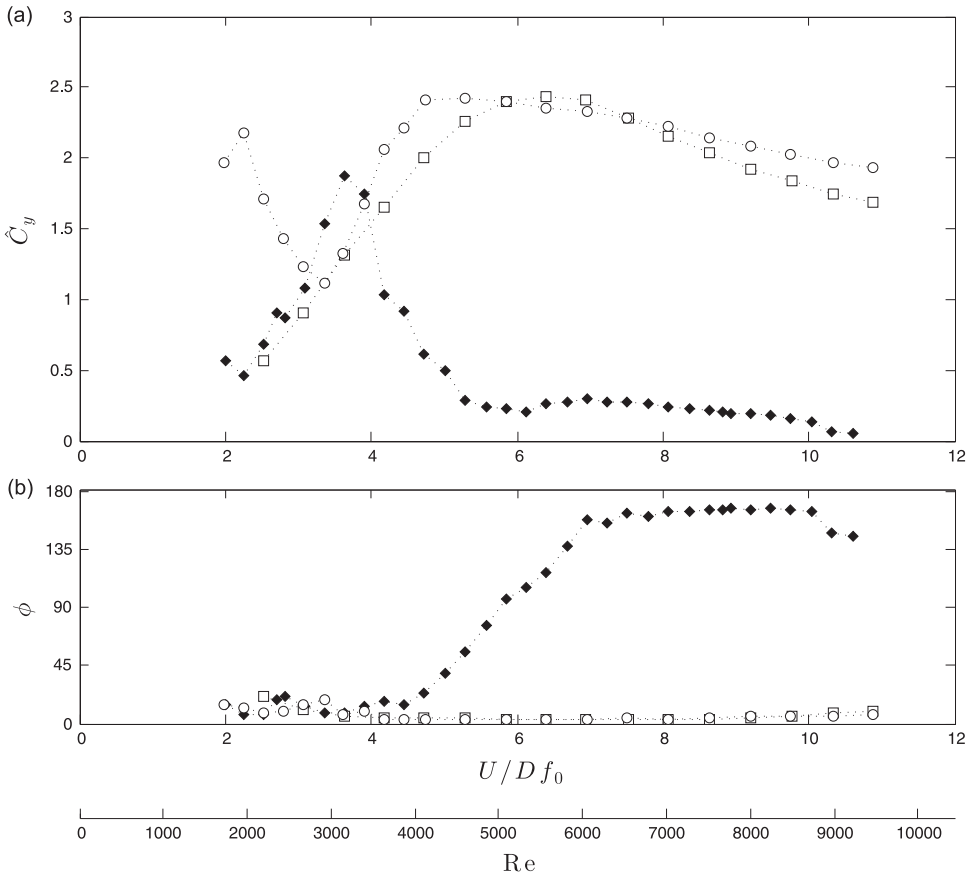

Fig. 7. (a) Amplitude of fluctuating lift coefficient and (b) phase angle versus reduced velocity. Key: ◇ plain cylinder VIV, □ solid splitter plate $L/D=0.5$, ○ solid splitter plate $L/D=1.0$.

with the $L/D=1.0$ showing a slightly lower response than the shorter plate. Displacement was physically limited to $\hat{y}/D=2.0$ by a stop in the rig; this was reached at around a reduced velocity 9 for the solid plates. Two runs have been performed for each solid device to verify repeatability, producing a small scatter in the data points for the highest amplitudes. The response of the slotted plate is qualitatively similar in the sense that no VIV was observed. However, the slope of the response versus reduced velocity is lower than that of the solid plates with $\hat{y}/D$ monotonically increasing with reduced velocity until $\hat{y}/D\approx 1.1$ is reached at the highest reduced velocities achieved in the experiments, a reduced velocity of almost 18.

Stappenbelt (2010) presents comparable results covering a wider range of plate lengths between $L/D=0.34$ and 4.0. He verified that the galloping response for splitter plates with $L/D<0.5$ terminated abruptly as reduced velocity was increased. In his investigation the maximum galloping response for $L/D=0.34$, 0.44 and 0.5 was $\hat{y}/D\approx 1.8$, 2.5 and 3.4 achieved for reduced velocities 15, 20 and 30, respectively. Stappenbelt also found that the slope of the initial response was not very different between splitter plates with $L/D=0.5$ and 1.0. This phenomenon has also been observed by Assi et al. (2014) to be occurring with other VIV suppressors with similar characteristic length.

The frequency responses in Fig. 5(b) also show that the cylinders fitted with splitter plates are not responding with VIV. Apart from a range of $U/Df_0<4$ the dominant frequencies of vibration for all devices are constant and significantly lower than that observed for the plain cylinder. The frequencies do not follow the Strouhal line for the plain cylinder during the typical upper branch of VIV. The solid plates appear to oscillate at more or less the same frequency, which is lower than that of the slotted plate; we shall return to this point later when discussing added mass.

The mean drag curves in Fig. 5(c) show no drag amplification for the cylinders with splitter plates during the equivalent synchronisation range of VIV. Although vibrating with much larger displacements, the splitter plates seem to keep drag below that observed during VIV of a plain cylinder. Results for the solid splitter plates show the same levels of drag as those reported by Stappenbelt (2010). The solid and the slotted plates, both having $L/D=1.0$, managed to reduce drag down to $\overline{C}_x\approx 1.0$ for the whole of the reduced velocity range. It is surprising that such large vibrations present considerably low drag; we shall return to this when discussing force decomposition. Stappenbelt (2010) also reports that drag continues to drop with increasing plate length for solid plates with $L/D>1.0$.

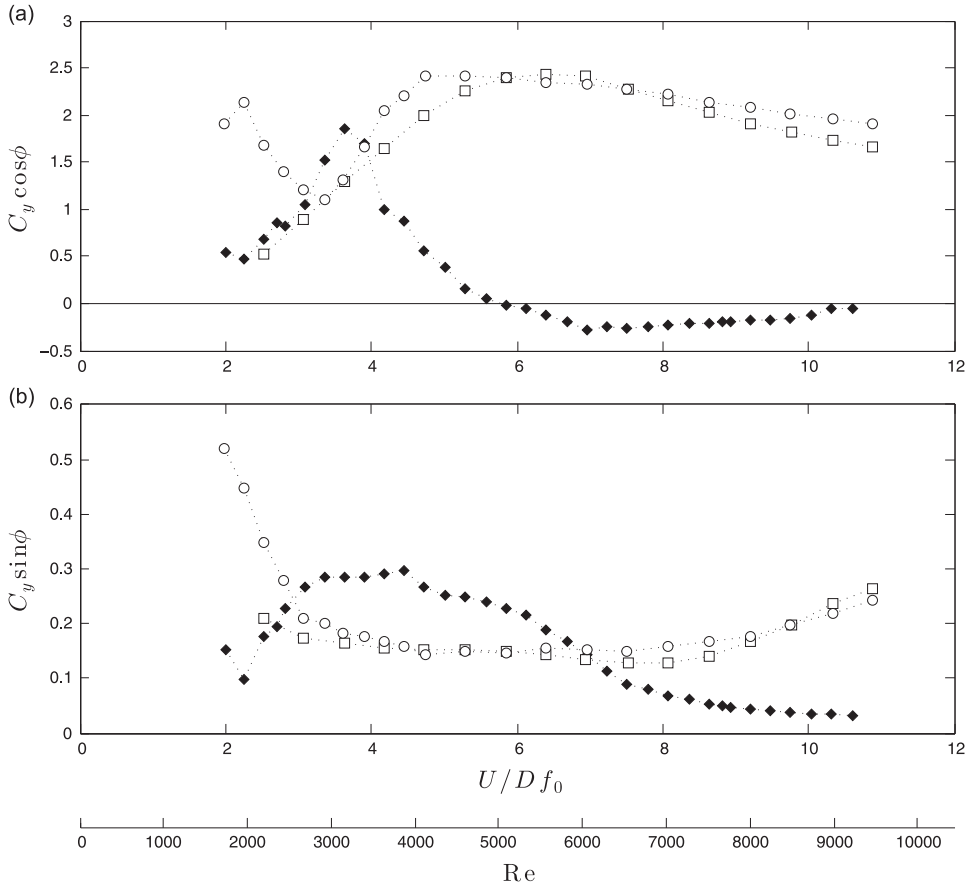

Fig. 8. Decomposition of lift coefficient in phase with (a) acceleration and (b) velocity. Key: ◊ plain cylinder VIV, □ solid splitter plate $L/D=0.5$, ○ solid splitter plate $L/D=1.0$.

3.2. Harmonic motion hypothesis: lift and phase angle

A careful analysis of the data acquired during each run revealed that response of the cylinder is quite well behaved, with a single dominant peak in the frequency spectrum and a fairly constant envelop of displacement. Fig. 6 presents a sample of the time series of displacement for a cylinder fitted with a $L/D=1.0$ splitter plate at $U/Df_0=8.1$. The continuous line represents the recorded displacement of the cylinder over time (t), while the dashed line represents a sine function with the corresponding frequency, f, and amplitude, $\hat{y}/D$, determined experimentally. It is clear that the movement of the cylinder can be approximated by such a simple harmonic function; the same was verified to occur for all plate configurations at all reduced velocities. Hence, a harmonic hypothesis for the movement is quite adequate.

Now, following the hypothesis for harmonic forcing and harmonic motion employed by Bearman (1984) and others, cross-flow displacement of the cylinder can be written simply as a sine function of time

$$y(t)=\hat{y}\sin(2\pi ft), \tag{1}$$

where $\hat{y}$ and f represent the harmonic amplitude and frequency of oscillation, respectively. The equation of motion for the second order harmonic oscillator is then

$$m\ddot{y}+c\dot{y}+ky=\left[\overline{C}_y+\hat{C}_y\sin(2\pi ft+\phi)\right]\tfrac{1}{2}\rho U^2D, \tag{2}$$

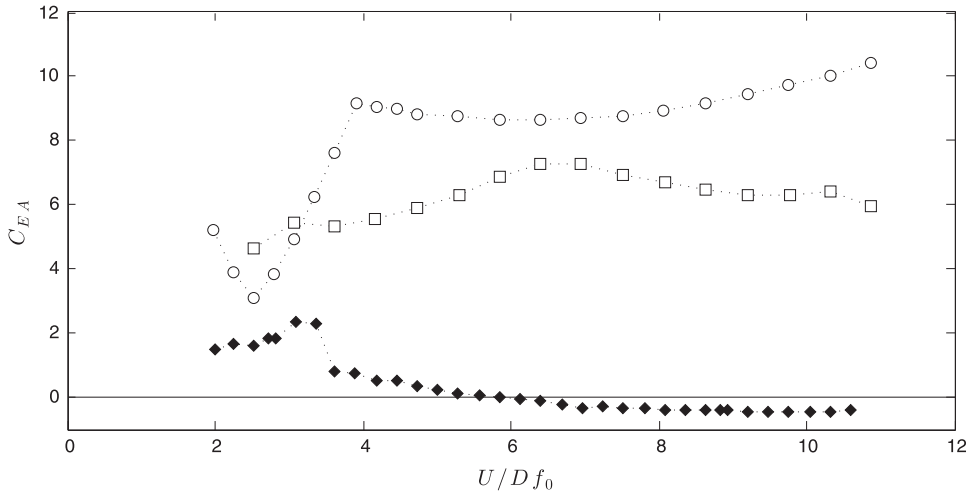

Fig. 9. Coefficient of effective added mass. Key: ◇ plain cylinder VIV, □ solid splitter plate $L/D=0.5$, ○ solid splitter plate $L/D=1.0$.

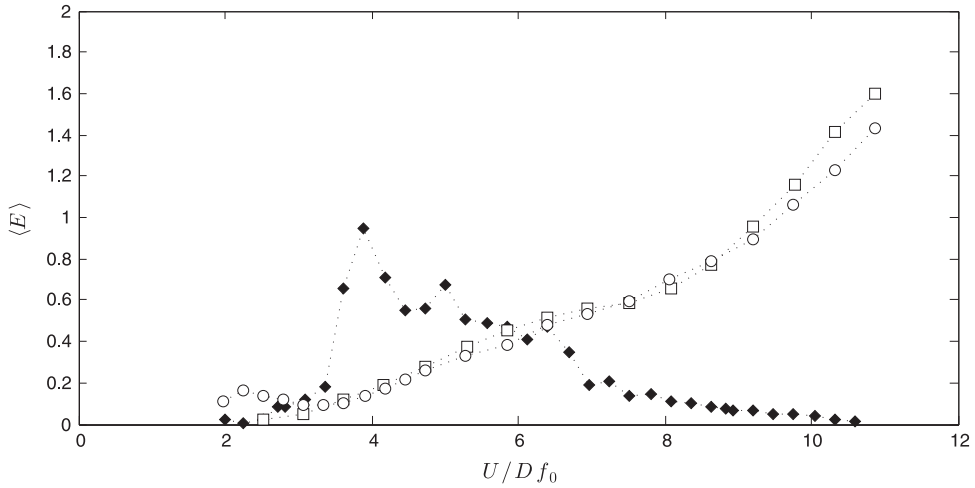

Fig. 10. Energy transferred from the flow to the body during one cycle of oscillation. Key: ◇ plain cylinder VIV, □ solid splitter plate $L/D=0.5$, ○ solid splitter plate $L/D=1.0$.

with the respective structural parameters of mass, m, stiffness, k, and damping, c. Displacement, y, velocity, $\dot{y}$, and acceleration, $\ddot{y}$ of the body and fluid force coefficients are time dependent and all terms are expressed per unit length of the cylinder. The fluid force and the body response oscillate at the same frequency f under a steady-state regime.

The total fluid force, on the right-hand side of Eq. (2) can then be divided into a time-average term $\overline{C}_y$ (usually equal to zero for symmetric cross sections) and a transient term modelled as a sine wave with amplitude $\hat{C}_y$ and frequency f, with ϕ representing the phase angle between displacement and force. In the present work $\hat{C}_y$ was determined by taking the r.m.s. of lift and multiplying it by $\sqrt{2}$, while ϕ was determined by means of a Hilbert transform applied to the time series of force and displacement, as explained in Khalak and Williamson (1999) and Assi (2009).

For body excitation to occur ϕ must be between 0° and 180°. A phase angle equal to either 0° or 180° means that no energy is transferred from the flow to the structure to excite any vibration. As far as the excitation is concerned, Bearman

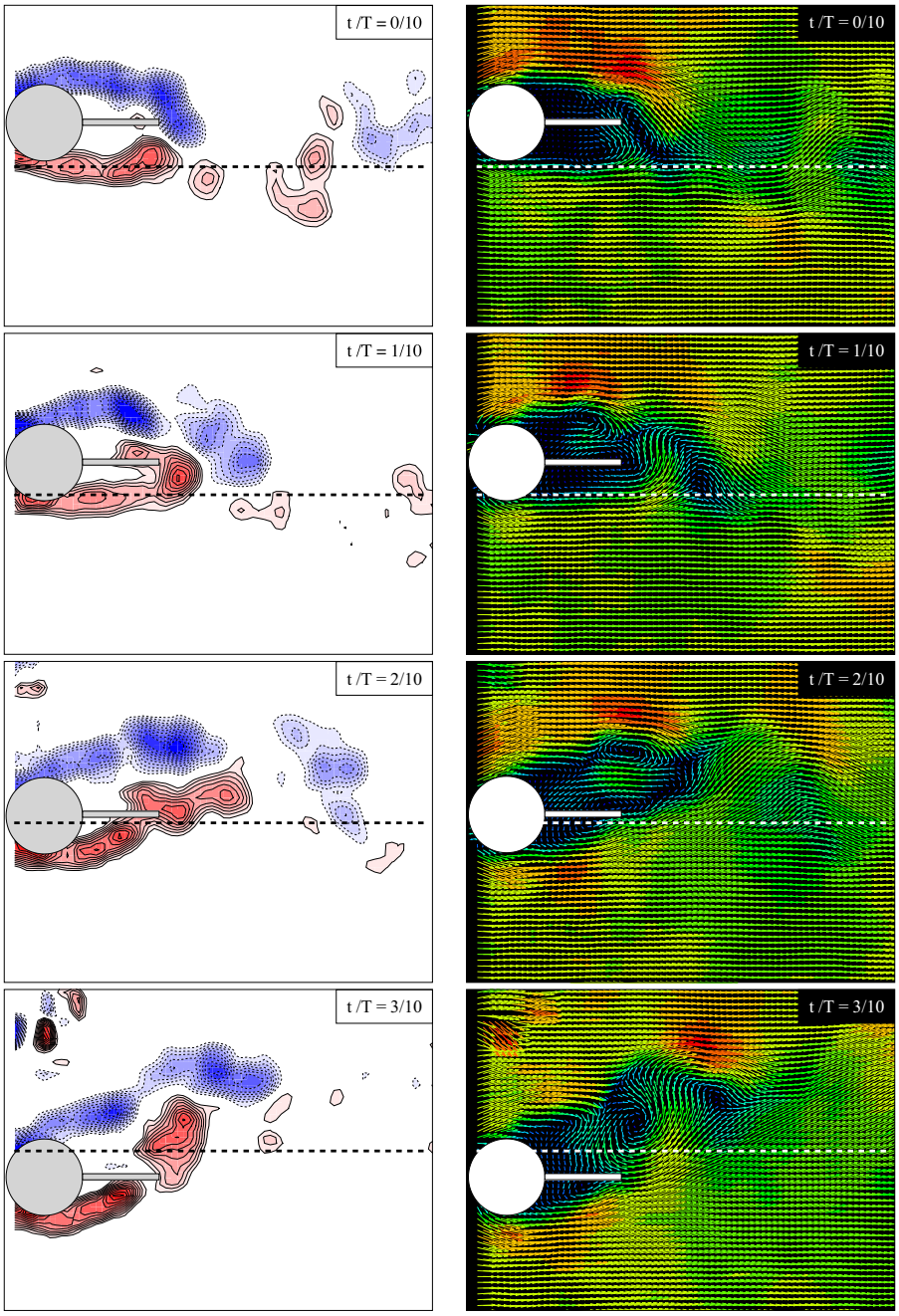

Fig. 11. Instantaneous fields of (left column) vorticity contours coloured by intensity and (right column) velocity vectors coloured by magnitude during one cycle of oscillation. $U/Df_0 = 6.4$ and $\mathrm{Re} = 4800$. A horizontal dashed line represents the centreline of the wake.

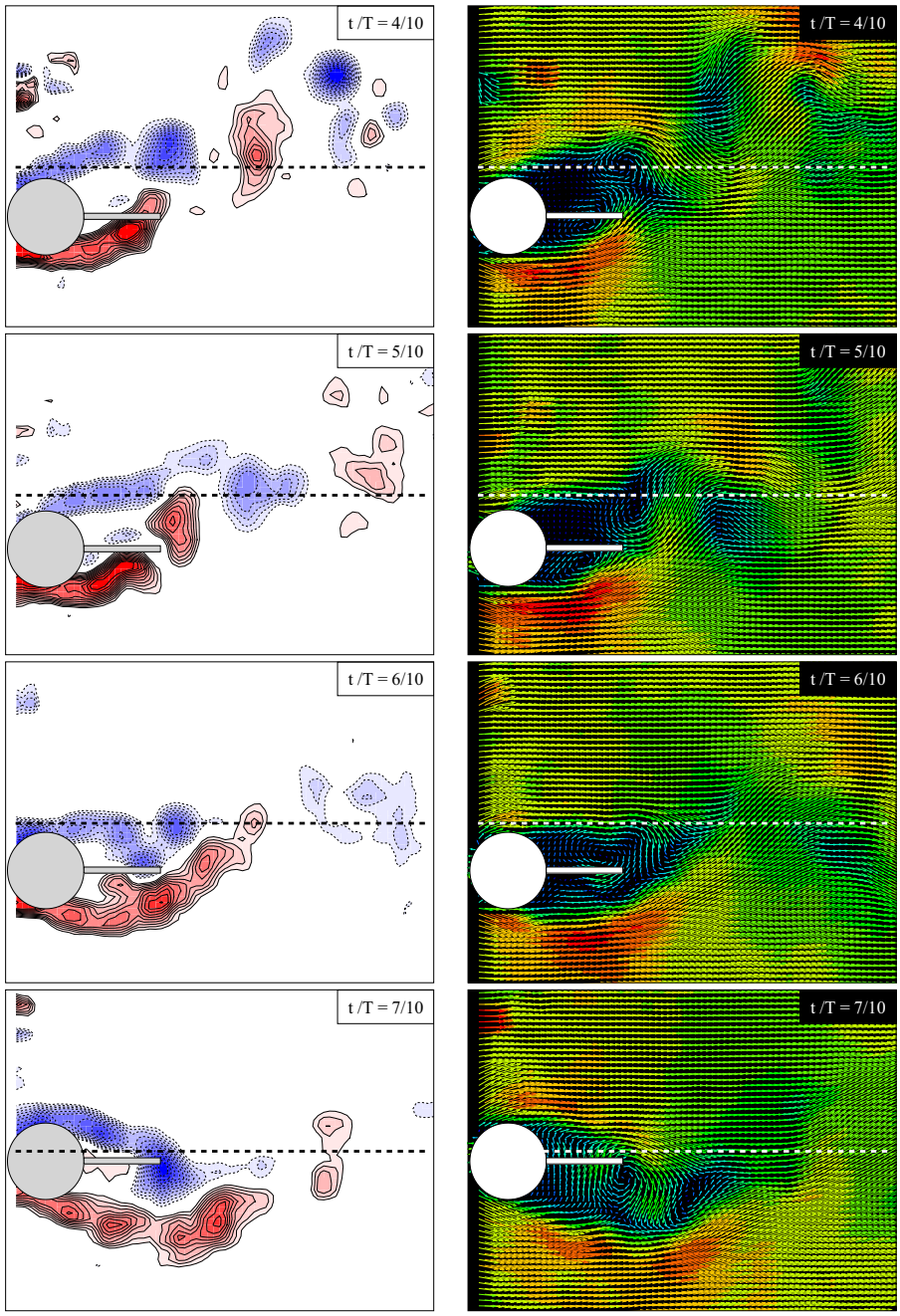

Fig. 11. (*continued*)

(1984) explains that "it is clear that the phase angle ϕ plays an extremely important role. The amplitude response does not depend on $\hat{C}_y$ alone but on that part of $\hat{C}_y$ in phase with the body velocity. Hence, measurements of the sectional fluctuating lift coefficient on a range of stationary bluff-body shapes will give little indication of the likely amplitudes of motion of similar bodies flexibly mounted". With VIV excitation, when reduced velocity is increased, ϕ shifts from almost 0° to almost 180° as the response passes through resonance. Khalak and Williamson (1999) clearly show, for a plain circular cylinder, how this phase shift is related to different wake modes and transitions between branches of response.

Fig. 7(a) presents results for $\hat{C}_y$ for the plain cylinder compared with the cylinder fitted with solid splitter plates. During the typical VIV response we notice the plain cylinder experiences a lift amplification close to the peak of resonance (at $U/Df_0 \approx 4$) before a considerable drop in $\hat{C}_y$ that remains for the rest of the synchronisation range. The cylinders with splitter plates, on the other hand, show a build-up of $\hat{C}_y$ at low values of reduced velocity, reaching a maximum of $\hat{C}_y \approx 2.5$ and then reducing slowly for $U/Df_0 > 6$. (Note: Uncertainties for force measurements are larger at low Re due to the small

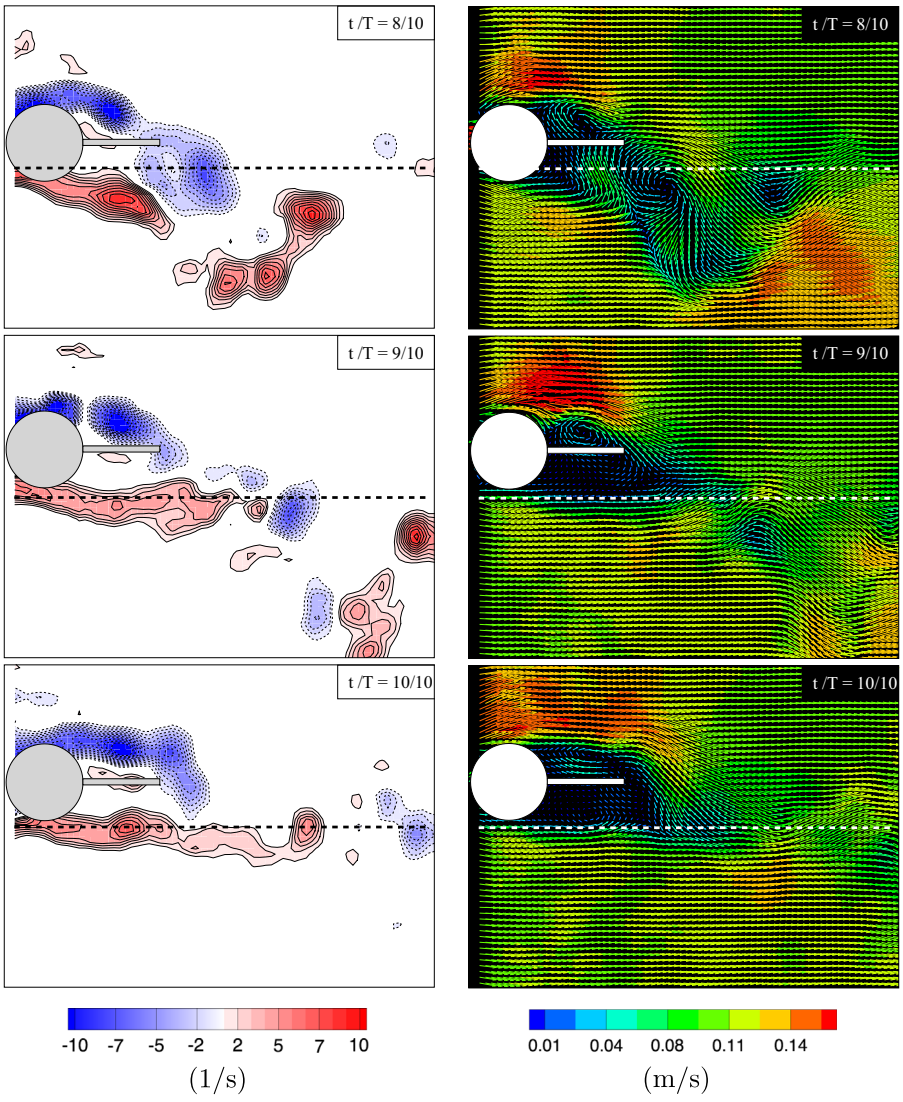

Fig. 11. (*continued*)

magnitude of measured forces, thus results for $\hat{C}_y$ and ϕ must be taken with caution for $U/Df_0 < 3$. To offer an estimate, uncertainties in $\hat{C}_y$ vary in approximate bands of: 15% for $U/Df_0 < 3$; 5% for $3 < U/Df_0 < 6$; and 1% for $U/Df_0 > 6$.) It is evident that the $\hat{C}_y$ curve for the resonant mechanism of VIV is qualitatively different from those for the hydrodynamic instability of galloping, but the difference between the phenomena is made clearer from measurements of ϕ presented in Fig. 7(b).

While the resonant response of VIV presents a phase shift of almost 180° when the response crosses the resonance peak (between $U/Df_0 = 4$ and 7). The galloping response of the solid plates experiences no such shift in ϕ, proving that the excitation mechanism is not of a resonant type. For the solid splitter plates C_y was not found to be *in phase* with velocity, otherwise ϕ would have been at values close to 90° in Fig. 7. Instead, ϕ remains at low values for the whole of the galloping response range with lift leading the movement of the cylinder by a very small time lag. This small value of ϕ, coupled with high values of C_y, provides the excitation to overcome the very-low structural damping of the system and induces high-amplitude galloping vibrations.

3.3. Added mass and energy transfer

In order to investigate further the system dynamics and the energy transfer from the flow to the body we calculate the components of the fluid lift force in phase with $\dot{y}$ and in phase with $\ddot{y}$. Fig. 8(a) presents $C_y \cos\phi$, the portion of the fluid force in phase with acceleration; as discussed in detail by Sarpkaya (2004) this takes the form of inertia and can also be considered as being directly related to the added mass of fluid. For a body subjected to FIV the *effective* added mass will be

different from the potential added mass (equal to the mass of displaced fluid for a circular cross section) or even the measured added mass of a cylinder in still water. For the VIV response of a plain cylinder it is known (Bearman, 1984) that the added mass coefficient will find its maximum at the resonance peak and become negative as the response passes through the synchronisation range as shown in Fig. 8(a). This will have an effect on the frequency response signature of VIV. However, $C_y \cos\phi$ for the splitter plates shows a different behaviour reaching much higher values and never becoming negative, once more demonstrating the absence of a resonant VIV-type mechanism. Khalak and Williamson (1999), for example, suggested that this effective added mass coefficient can be represented by

$$C_{EA} = \frac{1}{2\pi^3} \frac{C_y \cos\phi}{\hat{y}/D} \left[\frac{U}{Df}\right]^2, \tag{3}$$

taking into account the reduced velocity, amplitude and frequency of vibration. (Note that Khalak and Williamson (1999) define C_{EA} with a natural frequency measured in still water, which is cancelled out in the equation above.)

Values of C_{EA} are presented in Fig. 9. It is clear that the effective added mass coefficients of galloping cylinders with splitter plates are significantly greater than that of a plain cylinder in VIV. The splitter plate with $L/D = 1.0$ presents higher C_{EA} than the shorter one, and this is consistent with the lower frequencies of response observed for the galloping cylinder with splitter plates in Fig. 5(b).

Fig. 8(b) presents $C_y \sin\phi$, the portion of the fluid force in phase with velocity, which gives an idea of the excitation (or energy transfer) in the system. The VIV response exhibits positive values of $C_y \sin\phi$ during the synchronisation range, again with a maximum value found at the peak of resonance ($U/Df_0 \approx 4$). The galloping responses, on the other hand, show a very different behaviour with a broad minimum around $U/Df_0 = 5$ and increasing $C_y \sin\phi$ as reduced velocity is further increased. Based on the theory of second order oscillators, one can present the average non-dimensionalised energy transferred from the flow to the body during one cycle of oscillation, $\langle E \rangle$, as

$$\langle E \rangle = \pi \frac{\hat{y}}{D} C_y \sin\phi, \tag{4}$$

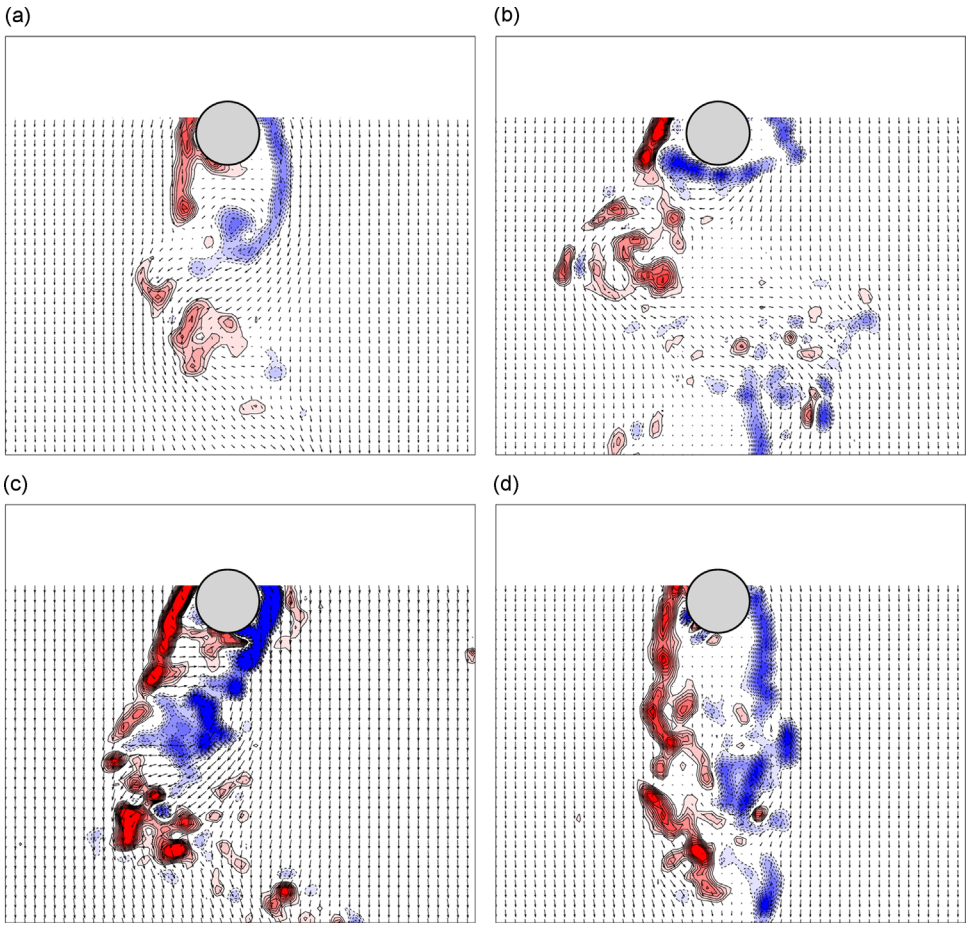

Fig. 12. Instantaneous vorticity contours and velocity vectors for a single cylinder at various reduced velocities: (a) $U/Df_0 = 3.0$, (b) 5.0, (c) 7.3 and (d) 12.

i.e. the work done by the non-dimensional hydrodynamic force in phase with velocity ($C_y \sin\phi$) during one cycle of non-dimensional displacement ($\hat{y}/D$). Results for $\langle E^* \rangle$ presented in Fig. 10 show that the plain cylinder VIV has its maximum energy transfer during synchronisation, as expected, but for the cylinder with splitter plates the energy transfer builds up as reduced velocity is further increased. It becomes evident that adding the splitter plates to the cylinder produces a much more energetic mechanism for vibration that is not of a resonant kind.

Due to a technical fault C_y was not measured for the cylinder with a slotted plate. Nevertheless, one may expect that the porosity of the plate will have an effect on the added mass and also the hydrodynamic damping which will influence the hydrodynamic excitation. Theoretically, the ideal-flow added mass coefficient for a slotted plate in still water should fall between values for the short and the long solid plates. The solidity of the plate is also expected to have an effect on flow behaviour in the near wake. Although communication between the shear layers might be inhibited, some flow between the two sides of the near wake is permitted through the slots. The slots on the plate may also help to dissipate energy as the flow is forced to pass through the narrow passages as the body oscillates. Flow visualisations presented in the next section will help to clarify various conjectures regarding the flow with solid and slotted splitter plates. However, the main conclusion is that the galloping response of the slotted plate is different from that of the solid plate of similar length, showing, for a given reduced velocity, lower amplitude of vibration at a higher frequency of oscillation (Fig. 5).

4. Flow field measurements

Measurements of the velocity field by PIV were taken on a horizontal plane at mid-length of the cylinder. The objective was to investigate the separated shear layers reattaching on the splitter plates as the cylinder moved across the flow. First we shall focus on the detailed visualisations of the flow around a solid splitter plate with $L/D=1.0$ before comparing velocity fields for the various plates.

Fig. 11 presents the evolution in time of the flow around a cylinder fitted with a solid splitter plate of $L/D=1.0$ during one cycle of oscillation at $U/Df_0 = 6.4$. The sequence is composed of 11 instantaneous flow fields identified in time by t/T, where $T = 1/f$ is the period of oscillation for that specific reduced velocity. The left column presents vorticity contours coloured by

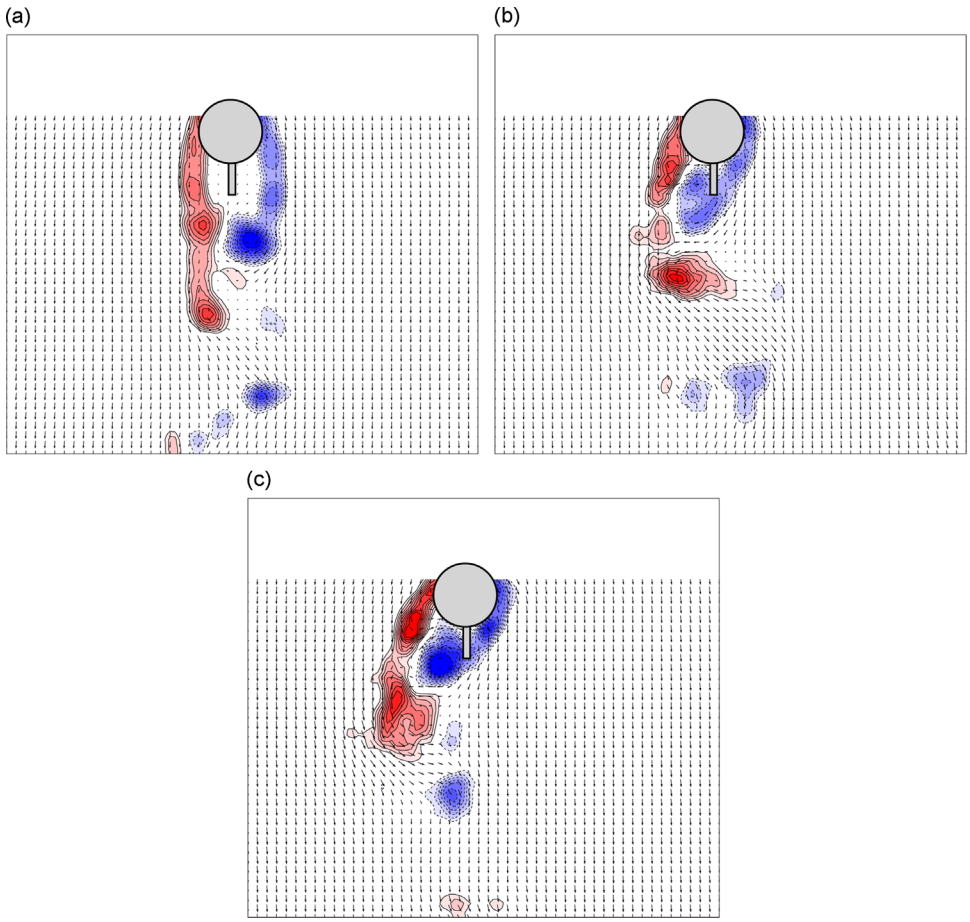

Fig. 13. Instantaneous vorticity contours and velocity vectors for a cylinder with a solid splitter plate $L/D=0.5$ at various reduced velocities: (a) $U/Df_0 = 3.0$, (b) 5.0 and (c) 7.3.

vorticity magnitude and the right column shows the corresponding velocity vectors coloured by velocity magnitude. At $t/T = 0/10$ the cylinder is in its uppermost position with $\dot{y} \approx 0$. The separated shear layers seem to be equally aligned with the flow direction, but relatively high speed flow is noticeable at the upper side of the cylinder (probably resulting from the previous cycle of oscillation). As time progresses, the cylinder moves down across the flow passing through the centreline with maximum $\dot{y}$ between $t/T = 2/10$ and 3/10. At this moment the shear layer on the lower side is drawn closer to the body and reattaches to the tip of the plate. The corresponding velocity field shows a recirculation bubble developed from the separation point on the cylinder to the reattachment point on the tip of the plate. This flow configuration generates a lift force in the same direction as the body movement, thus providing the excitation for galloping. A lift force with the same hydrodynamic origin was reported by Assi et al. (2009) in experiments with a free-to-rotate splitter plate. The cylinder reaches its lowermost position with $\dot{y} \approx 0$ at $t/T = 6/10$ when the reattaching shear layer seem to recover symmetry. On the way up, the cylinder crosses the centreline with maximum $\dot{y}$ between $t/T = 7/10$ and 8/10. The reattachment of the upper shear layer is now made possible by the strong $\dot{y}$.

During this cycle the cylinder is able to extract energy from the flow due to the reattachment of the shear layers on the plate, thus supporting the flow sketch proposed in Fig. 2. Vortex shedding is observed to occur downstream of the plate throughout the cycle, which might have an effect on the amount of lift generated on the body as well as the phase lag between the force and movement. The flow behaviour will vary as reduced velocity (and Reynolds number) is varied, especially as the reduced velocity moves away from the VIV synchronisation range in which vortex shedding may have a considerable influence.

Similar PIV measurements were carried out to investigate the flow around the cylinder with other plates. For brevity, we will only present results for the instant when the cylinder crosses the centreline for various reduced velocities. But first, Fig. 12 presents vorticity contours of the instantaneous wake generated around a plain cylinder in VIV to serve as a reference. (Note: Vorticity contours presented in the next figures are intended to offer a qualitative interpretation of the wake, therefore key for the colour scales, which vary with flow speed, is not necessary. The same applies to the velocity vectors.)

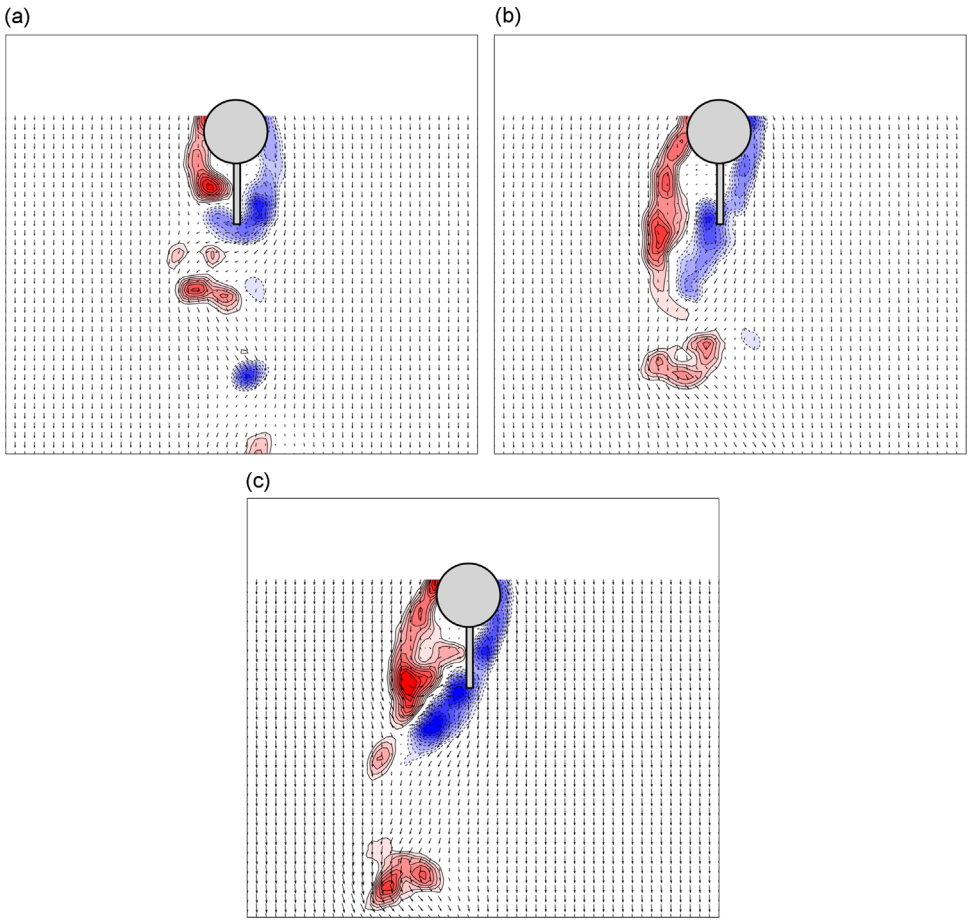

Fig. 14. Instantaneous vorticity contours and velocity vectors for a cylinder with a solid splitter plate $L/D = 1.0$ at various reduced velocities (a) $U/Df_0 = 3.0$, (b) 5.0 and (c) 7.3.

Reduced velocities of $U/Df_0 = 3.0$, 5.0, 7.3 and 12 are located within and just beyond the synchronisation range (identified with an asterisk in the axis of Fig. 5(a), for convenience). Data was acquired when the cylinder was crossing the centreline from left to right, therefore presenting maximum cross-flow velocity. It is possible to observe the evolution of the wake for the different branches of the VIV response. For reduced velocity 3.0 in Fig. 12(a) the cylinder presents small $\hat{y}/D$ with a typical '2S'-mode vortex wake being shed (Refer to Williamson and Govardhan, 2004 for a description of wake modes.) For reduced velocity 5.0 in Fig. 12(b), close to the peak of resonance, the '2P' wake appears much wider due to the high-amplitude movement of the cylinder. This wake changes mode again in the lower branch of vibration as shown for reduced velocity 7.3 in Fig. 12(c). For $U/Df_0 = 12$ the cylinder is no longer experiencing VIV excitation. For all cases in Fig. 12 the interaction of the separated shear layers in the vortex-formation mechanism is quite evident.

Fig. 13 presents the flow field around a cylinder with a solid splitter plate with $L/D = 0.5$ for the same reduced velocities as presented for the plain cylinder. At $U/Df_0 = 3.0$ the cylinder experiences very small movement across the flow and the galloping mechanism has not developed yet. But for the higher reduced velocities, the shear layer on the right-hand side of the cylinder is drawn closer to the plate as the cylinder moves with maximum $\dot{y}$ to the right; consequently, galloping is sustained. For the longer solid plate of $L/D = 1.0$, presented in Fig. 14, the separated shear layers manage to reattach to the tip of the plate for all three reduced velocities investigated. Galloping is incipient at $U/Df_0 = 3.0$ but it dominates the response for the higher reduced velocities. The instants captured in Fig. 14 are equivalent to $t/T = 2/10$ and 8/10 in Fig. 11. Although one may think the 1D-long plate would be able to extract more energy from the flow during the galloping mechanism it should be recalled that the responses of both plates in Fig. 5(a) are rather similar.

Results for the slotted splitter plate with $L/D = 1.0$ are not conceptually different from the others, as seen in Fig. 15. For $U/Df_0 = 3.0$ the vortex formation length is certainly extended due to the presence of the plate, but no reattachment of the shear layers on the plate is observed. For reduced velocities 5.0 and 7.3 a clear deflection of the wake is noticeable due to $\dot{y}$ and the shear layer on the right-hand side reattaches to the tip of the plate. The reduced rate of increase of response with reduced velocity allowed PIV measurements to be taken up to $U/Df_0 = 12$, where the same behaviour was observed. In summary, from Fig. 15 it becomes clear that a similar galloping mechanism is also driving the response of the slotted plate.

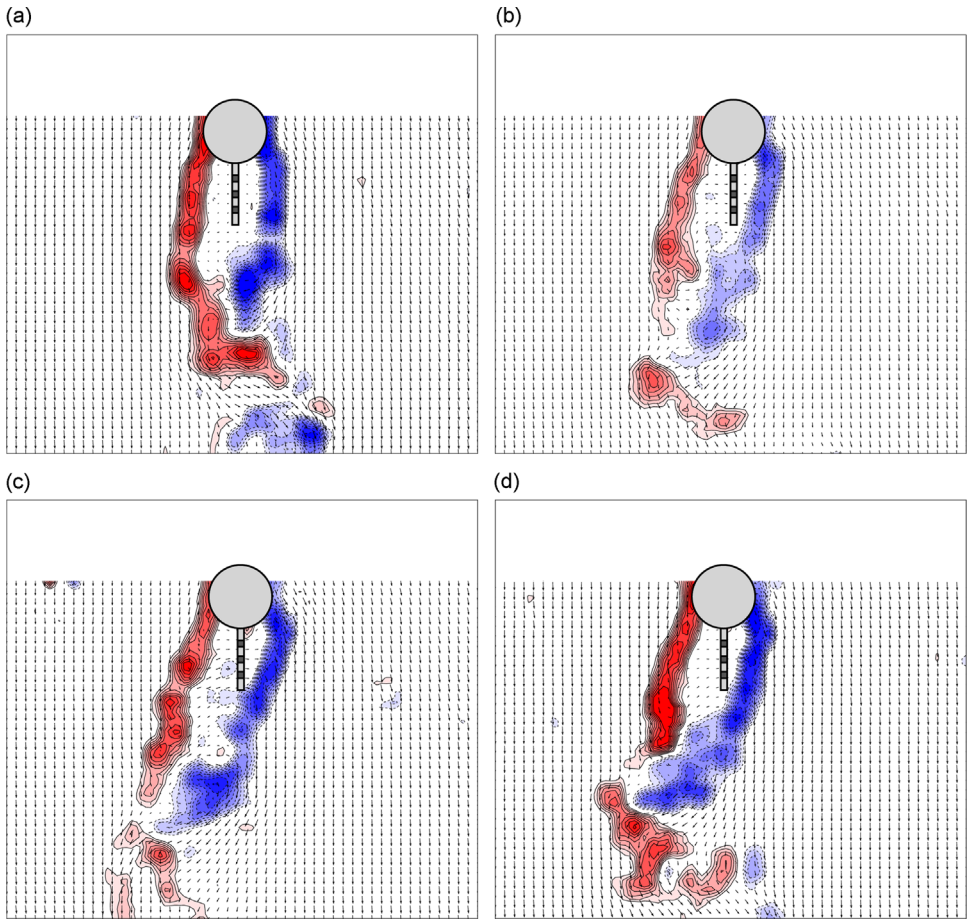

Fig. 15. Instantaneous vorticity contours and velocity vectors for a cylinder with a slotted splitter plate $L/D = 1.0$. (a) $U/Df_0 = 3.0$, (b) 5.0, (c) 7.3 and (d) 12.

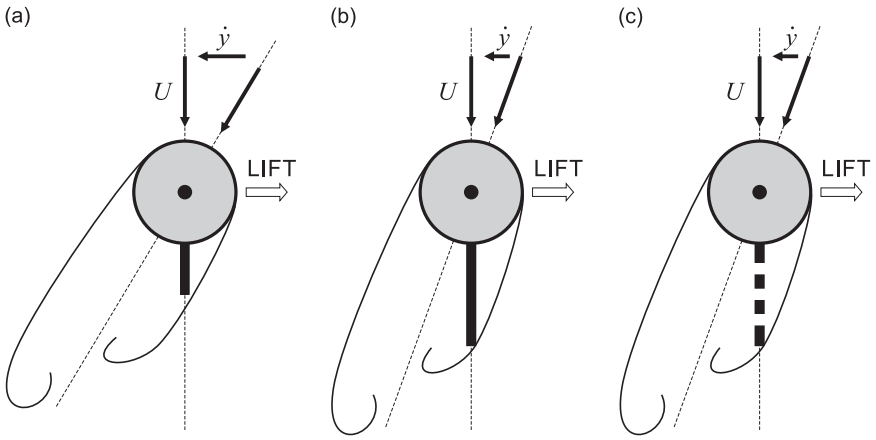

Fig. 16. Sketches of the hydrodynamic mechanism leading to the galloping instability of a cylinder with (a) a solid short splitter plate $L/D=0.5$, (b) a solid long splitter plate $L/D=1.0$ and (c) a slotted splitter plate $L/D=1.0$.

Note that the PIV measurements performed in the present work were not aimed at capturing the small flow scales within the recirculation bubble or through the slots. Also, flow fields presented in Figs. 12–15 were taken for the same reduced velocities, but the cylinders are oscillating at different frequencies for each case.

Independently of plate length or porosity, the general flow pattern that induces galloping is found to be the same, as summarised for all geometries in Fig. 16. At small amplitudes one shear layer moves close to the splitter plate while the opposing one moves away, hence producing a pressure difference across the plate. For larger amplitudes the shear layers intermittently reattach to the tip of a plate as the body oscillates. This reattachment sustains a pressure difference across the splitter plate feeding the excitation. In all cases, lift is generated on the cylinder/splitter plate combination.

Future investigations could focus on the plate solidity ratio to evaluate its effect on the response of bluff bodies with permeable structures in between the separated shear layers. Such a configuration may be useful for many engineering applications if shown that porous plates may be effective in suppressing vortex shedding and reducing drag without being prone to severe galloping, at least for moderate flow speeds.

5. Conclusion

In the present work we have investigated the FIV response of circular cylinders fitted with three different geometries of splitter plate. Hydrodynamic force decompositions together with PIV measurements of the flow field around the plates confirm that a transverse galloping mechanism is responsible for driving the cylinders with splitter plates into high-amplitude vibrations.

Firstly, this conclusion is supported by the overall behaviour of the response concerning a non-axisymmetric cross-section vibrating in 1-dof with displacements that monotonically increase with flow speed. Besides that, the driving mechanism is not resonant, since no phase shift between movement and forcing was observed as the frequency of vibration passes through the natural frequency of the system. Finally, flow visualization of the separated shear layers reattaching on the tip of the plates reveal the hydrodynamic mechanism that produces a transverse force in phase with the body's velocity.

Solid plates with $L/D=0.5$ and 1.0 showed a much larger increase in response with increasing reduced velocity than the slotted plate, indicating that they can extract more energy from the flow. The effect of the slots on excitation is thought to be twofold: they increase hydrodynamic damping and reduce the pressure difference across the splitter plate, but this requires further confirmation. Independently of plate length or porosity, the general flow pattern that induces galloping is found to be the same.

The validity of the quasi-steady theory of galloping has not been verified in the present study. Nakamura et al. (1994) have already pointed out that it might not hold true for circular cylinders fitted with long splitter plates. Simply modelling the lift force as an harmonic function may not be the most accurate approach, but it reveals distinct features of lift, phase angle, added mass and energy transfer, clearly isolating the nature of the galloping instability from the VIV response of a plain cylinder.

Acknowledgments

The authors wish to acknowledge the support of CAPES (2668-04-1) at the time of the experiments. GRSA is grateful to FAPESP (2013/07335-8) and CNPq (308916/2012-3) that allowed him time to revisit the data and write this paper.

References

Apelt, C.J., West, G.S., 1975. The effects of wake splitter plates on bluff-body flow in the range $10^4 < R < 5 \times 10^4$. Part 2. Journal of Fluid Mechanics 71, 145–160.

Apelt, C.J., West, G.S., Szewczyk, A., 1973. The effects of wake splitter plates on the flow past a circular cylinder in the range $10^4 < R < 5 \times 10^5$. Journal of Fluid Mechanics 61, 187–198.

Assi, G.R.S., 2009. Mechanisms for Flow-induced Vibration of Interfering Bluff Bodies (Ph.D. thesis). Imperial College London, London, UK, available from ⟨www.ndf.poli.usp.br/∼gassi⟩.

Assi, G.R.S., 2014a. Wake-induced vibration of tandem and staggered cylinders with two degrees of freedom. Journal of Fluids and Structures 50, 329–339.

Assi, G.R.S., 2014b. Wake-induced vibration of tandem cylinders of different diameters. Journal of Fluids and Structures 50, 340–357.

Assi, G.R.S., Bearman, P.W., Carmo, B., Meneghini, J., Sherwin, S., Willden, R., 2013. The role of wake stiffness on the wake-induced vibration of the downstream cylinder of a tandem pair. Journal of Fluid Mechanics 718, 210–245.

Assi, G.R.S., Bearman, P.W., Kitney, N., 2009. Low drag solutions for suppressing vortex-induced vibration of circular cylinders. Journal of Fluids and Structures 25, 666–675.

Assi, G.R.S., Bearman, P.W., Kitney, N., Tognarelli, M., 2010a. Suppression of wake-induced vibration of tandem cylinders with free-to-rotate control plates. Journal of Fluids and Structures 26, 1045–1057.

Assi, G.R.S., Bearman, P.W., Meneghini, J., 2010b. On the wake-induced vibration of tandem circular cylinders: the vortex interaction excitation mechanism. Journal of Fluid Mechanics 661, 365–401.

Assi, G.R.S., Bearman, P.W., Rodrigues, J., Tognarelli, M., 2011. The effect of rotational friction on the stability of short-tailed fairings suppressing vortex-induced vibrations. in: Proceedings of OMAE2011, 30th International Conference on Ocean, Offshore and Arctic Engineering, Rotterdam, The Netherlands.

Assi, G.R.S., Bearman, P.W., Tognarelli, M., 2014. On the Stability of a Free-To-Rotate Short-Tail Fairing and a Splitter Plate as Suppressors of Vortex-Induced Vibration, Ocean Engineering, TBA.

Bearman, P.W., 1965. Model with a blunt trailing edge and fitted with splitter plates. Journal of Fluid Mechanics 21, 241–255.

Bearman, P.W., 1984. Vortex shedding from oscillating bluff bodies. Annual Review of Fluid Mechanics 16, 195–222.

Bearman, P.W., Gartshore, I.S., Maull, D.J., Parkinson, G.V., 1987. Experiments on flow-induced vibration of a square-section cylinder. Journal of Fluids and Structures 1, 19–34.

Blevins, R., 1990. Flow-Induced Vibration, second edition Van Nostrand Reinhold, New York.

Chang, C.-C., Kumar, R., Bernitsas, M.M., 2011. VIV and galloping of single circular cylinder with surface roughness at $3.0 \times 10^4 \leq \mathrm{Re} \leq 1.2 \times 10^5$. Ocean Engineering 38 (16), 1713–1732.

Cimbala, J., Garg, S., 1991. Flow in the wake of a freely rotatable cylinder with splitter plate. AIAA Journal 29, 1001–1003.

den Hartog, J., 1956. Mechanical Vibrations, fourth edition McGraw Hill, New York.

Gerrard, J., 1966. The mechanics of the formation region of vortices behind bluff bodies. Journal of Fluid Mechanics 25, 401–413.

Khalak, A., Williamson, C.H.K., 1999. Motions, forces and mode transitions in vortex-induced vibrations at low mass-damping. Journal of Fluids and Structures 13, 813–851.

Nakamura, Y., Hirata, K., Kashima, K., 1994. Galloping of a circular cylinder in the presence of a splitter plate. Journal of Fluids and Structures 8, 355–365.

Nakamura, Y., Hirata, K., Urabe, T., 1991. Galloping of rectangular cylinders in the presence of a splitter plate. Journal of Fluids and Structures 5, 521–549.

Naudascher, E., Rockwell, D., 1994. In: Balkema, A.A. (Ed.), Flow-Induced Vibrations, An Engineering Guide, Rotterdam. 1st Edition.

Paidoussis, M., Price, S., deLangre, E., 2011. Fluid-Structure Interactions: Cross-Flow-Induced Instabilities, 1st Edition Cambridge University Press, New York.

Parkinson, G., 1971. Wind-induced instability of structures. Philosophical Transactions of the Royal Society 269, 395–413.

Parkinson, G., 1989. Phenomena and modelling of flow-induced vibrations of bluff bodies. Progress in Aerospace Sciences 26, 169–224.

Roshko, A., 1954. On the Drag and Shedding Frequency of Two-dimensional Bluff Bodies. Technical Report. TN-3169, NACA.

Sarpkaya, T., 2004. A critical review of the intrinsic nature of vortex-induced vibrations. Journal of Fluids and Structures 19, 389–447.

Stappenbelt, B., 2010. Splitter-plate wake stabilisation and low aspect ratio cylinder flow-induced vibration mitigation. International Journal of Offshore and Polar Engineering 20 (3), 1–6.

Unal, M., Rockwell, D., 1987. On vortex formation from a cylinder. Part 2. Control by splitter-plate interference. Journal of Fluid Mechanics 190, 513–529.

Williamson, C.H.K., Govardhan, R., 2004. Vortex-induced vibrations. Annual Review of Fluid Mechanics 36, 413–455.